

A new perspective on staurolite crystal chemistry: Use of stoichiometric and chemical end-members for a mole fraction model

M. J. HOLDAWAY, B. MUKHOPADHYAY

Department of Geological Sciences, Southern Methodist University, Dallas, Texas 75275, U.S.A.

M. D. DYAR

Department of Geological Sciences, University of Oregon, Eugene, Oregon 97403, U.S.A.

B. L. DUTROW

Department of Geology, University of Iowa, Iowa City, Iowa 52242, U.S.A.

DOUGLAS RUMBLE III

Geophysical Laboratory, 5281 Broad Branch Road NW, Washington, DC 20015-1305, U.S.A.

J. A. GRAMBLING

Department of Geology, University of New Mexico, Albuquerque, New Mexico 87131, U.S.A.

ABSTRACT

Recent contributions to the crystal chemistry of staurolite have been aided by Mössbauer studies on 35 natural and synthetic samples and structure determinations on 42 single crystals. The combination of these data with chemical studies enables us to understand better the crystal chemistry of this mineral relative to its use as a petrogenetic indicator. In reduced rocks about 3.5% of Fe is Fe³⁺, and in oxidized rocks about 7% is Fe³⁺. It is now possible to recast a staurolite chemical analysis in terms of site occupancies using reasonable guidelines and intersite partitioning. Whereas the formula for hypothetical stoichiometric end-member iron staurolite is H₂Fe₄Al₁₈Si₈O₄₈, chemical end-member formulas such as H₃Fe_{4.35}Al_{17.90}Si_{7.65}O₄₈ are useful for retrieving thermodynamic data from experimental studies on simple systems. Other formulas may be written to account for appropriate amounts of the R²⁺H₋₂ substitution. In the absence of analyses for H, stoichiometry may be estimated from chemical analyses by assuming Si + Al = 1/3 Li + 2/3 Ti + Fe³⁺ = 25.55 ions pfu. In normal staurolite Li may be assumed to be 0.2. H may then be estimated by subtracting total cation charge from 96. H estimates for any group of related natural staurolite samples are normally a function of mineral assemblage. The preferred thermodynamic mole fraction (activity) model for phase equilibrium calculations takes into account dilution on all cation sites except H. Applied to staurolite-chloritoid pairs, this mole fraction model does not provide an explanation for the variable K_d values between these two minerals. Knowledge of the ferric content, formula, and mole fraction model of staurolite enables meaningful retrieval and use of thermochemical quantities from experimental studies.

INTRODUCTION

Staurolite, a common silicate of amphibolite facies pelitic schists, has the potential to provide useful information on temperature (*T*), pressure (*P*), and *X*_{H₂O}. However, because of its complex crystal chemistry, petrologists have had mixed success in extracting meaningful information on these intensive variables. The problem is illustrated in several ways: (1) the lack of agreement concerning the formula of staurolite; (2) the lack of a satisfactory activity model; (3) the disagreement between *T* measurements predicted from experimental results on staurolite and those indicated by other equilibria such as garnet-biotite geothermometry (e.g., Pigage and Greenwood, 1982; Lang and Rice, 1985; Holdaway et al., 1988); and (4) the reversals in Fe-Mg *K*_d values for staurolite-

garnet (Schreyer et al., 1984; Balleve et al., 1989) and for staurolite-chloritoid (Grambling, 1983).

In recent years, a number of significant observations have been made on staurolite that will ultimately help us to solve the problems of this mineral. These include (1) the determination that Li is an important constituent of many staurolite samples (Grew and Sandiford, 1984; Dutrow et al., 1986), (2) the realization that staurolite varies in H content according to a vacancy substitution that involves R²⁺ ions (Lonker, 1983; Holdaway et al., 1986a, 1986b), and (3) the experimental determination of the stability of an iron staurolite with about three H atoms (Dutrow and Holdaway, 1989).

Until recently, a comprehensive study of the Fe³⁺-Fe²⁺ chemistry of staurolite has been lacking. Consequently,

there has been some uncertainty regarding the amount and behavior of Fe^{3+} (e.g., Holdaway et al., 1986a). In part this results from the difficulty encountered when attempting to digest staurolite in acidic solution and maintain the Fe oxidation states for wet chemical analysis (J. Husler, personal communication). In addition, most previous Mössbauer studies have been conducted on a small number of incompletely characterized specimens, and they have yielded equivocal results (see references in Dyar et al., 1991). Dyar et al. (1991) have completed Mössbauer spectroscopy on 23 well-characterized natural staurolite samples and 12 synthetic samples. This has enabled a determination of the approximate Fe^{3+} content of each specimen, and the large population studied allows site assignments for Fe^{2+} and Fe^{3+} that have a higher degree of certainty than has previously been possible.

Whereas a number of structural studies have been undertaken on staurolite (e.g., Smith, 1968; Tagai and Joswig, 1985; Ståhl et al., 1988; Alexander, 1989), only now has a study examined the structure of a large number of staurolite samples. Hawthorne et al. (manuscripts a and b, in preparation; see also Hawthorne et al., 1991) have determined the structure of 42 single crystals from 17 staurolite samples. By carefully considering how the chemistry of each single crystal affects site occupancies and site dimensions, Hawthorne and his coworkers have made a major contribution to our understanding of the crystal chemistry of staurolite.

In this paper, we attempt to resolve some of the remaining crystal chemical problems for staurolite using mainly chemical data of Holdaway et al. (1986a, 1986b) and Dutrow et al. (1986); Mössbauer results, interpretations, and chemical data of Dyar et al. (1991); and structural, chemical, and crystal chemical results of Hawthorne et al. (manuscripts a and b, in preparation). Our primary intent in this research is to provide approaches that may be used to help determine meaningful chemical formulas, activity models, molar volumes, thermochemical data, and mixing parameters for natural staurolite. Our goal is to provide the petrologist with useful tools with which to estimate T , P , or $X_{\text{H}_2\text{O}}$ in staurolite-bearing rocks. In undertaking this task, some assumptions must still be made. For example, the behavior of minor elements Ti and Mn in staurolite is still largely unknown. However, most of the assumptions that are needed at this stage concern second order effects that can be accounted for in one of several ways without changing the results. For such uncertainties, we will use the simplest model that explains the observations. For a given staurolite, an X-ray structure refinement may reveal a more precise crystal chemistry than proposed here, but the petrologist would not be able to determine such precise site occupancies without a detailed structure determination for each staurolite under consideration.

Fe^{3+} CONTENT OF STAUROLITE

In evaluating the Fe^{3+} content of staurolite, we will emphasize the results on natural staurolite because the sam-

TABLE 1. Silicates, oxides, and oxide compositions coexisting with staurolite, where available

Specimen	Silicates,* etc.	Fe-Ti oxides**	Staurolite percent Fe^{3+} of total Fe†
3-3	Bt-Gt-Chl-Crd-And	Hem ₀	3
53-2	Bt-Gt-Sil-Gr	Hem ₀	3
203	Bt-Gt-Chl-And-Gr	Hem ₀	3
6-3	Bt-Gt-Sil-Pl	Hem ₀	5
114-1	Bt-Gt-Chl-Gr	Hem ₁	3
71-62R	Chl-Cld	Hem ₂ -Mag	3
HV-10	Bt-Gt-Ky-Pl-Po	Hem ₁	3
71-60E	Chl-Cld	Hem ₆ -Mag	3
71-62U	Chl-Cld-Ky	Hem ₁₀ -Mag	3
HV-116	Bt-Gt-Pl	Hem ₁₀ -Mag	7
71-62B	Cld-Ky	Hem ₁₁ -Hem ₇₃ -Mag	3
356-1	Bt-Gt-Chl-Pl-Ep-Gr	Hem ₁₂ -Mag	3
HV-4	Bt-Gt-Chl-Pl	Hem ₁₂ -Mag	6
71-62T	Chl-Cld-Ky	Hem ₁₂ -Hem ₇₁ -Mag	3
HV-112	Bt-Gt-Pl	Hem ₁₄ -Mag	9
ER-70	Bt-Gt	Ilm	6
77-55C	And	Ilm	7
82TP9A	Bt-Gt-And	Hem ₇₁ -Mag	9
92TP9	Bt-Gt-And	Hem ₇₂	8
EH-6	Bt-Gt-Chl-Sil-Ged-Cum-Crn	Mag	12

* Plus Qtz-Ms, except EH-6.

** Hematite component in ilmenite; where compositions are not available, oxides are indicated by abbreviations.

† Values at 3% represent a threshold estimate; Mössbauer doublet for Fe^{3+} was not resolved (Dyar et al., 1991).

ple size was larger and the results more precise than for the synthetic material (Dyar et al., 1991). In addition, the synthetic staurolite was produced at much higher pressures than those at which the natural specimens grew. These Mössbauer results have a $\pm 3\%$ absolute error. In 13 of the 23 natural staurolite samples analyzed, no Fe^{3+} (doublet 5) was resolved. Dyar et al. (1991) inferred an Fe^{3+} content of 3% of the total Fe for such staurolite, because the minimum detectable amount is 4% in such complex spectra. Staurolite, like biotite (Dyar, 1990; Guidotti and Dyar, 1991) and garnet (M. D. Dyar, unpublished data), probably contains some Fe^{3+} even under reducing conditions. We emphasize that some of these specimens may have less than 3% Fe^{3+} , and others may well have more, because only five of the six observed doublets were ever resolved in any given specimen, and the smallest resolved doublet corresponded to 8–10% of the Fe in these specimens. This indicates that some of these staurolite samples with unresolved doublet 5 could have as much as 7% of Fe as Fe^{3+} .

The natural staurolite samples may be broadly grouped into two categories according to Fe^{3+} content (Dyar et al., 1991): 17 with 3–6% of Fe as Fe^{3+} , which commonly coexist with an ilmenite (\pm magnetite) containing 0–12% hematite component, and six with 7–12% of Fe as Fe^{3+} , which commonly coexist with ilmenite or hematite (\pm magnetite) containing 10–72% hematite component. Table 1 shows that of staurolite coexisting with Fe-Ti oxide, ten coexisting with Hem _{≤ 10} average 3.5% Fe^{3+} and ten coexisting with Hem _{> 10} or magnetite (or ilmenite of unknown composition) average 7% Fe^{3+} . These data may

TABLE 2. Average stoichiometry (48 O atom basis) of 31 complete staurolite analyses with low Fe³⁺*

Element(s)	Range	Average**	Std. dev.
Si	7.49–7.81	7.64	0.07
Al	17.53–18.03	17.80	0.13
Ti	0.08–0.15	0.11	0.02
Fe ²⁺	1.74–3.34†	2.98†	0.41†
Fe ³⁺	0.08–0.20‡	0.10‡	0.02‡
Mg	0.28–1.10	0.69	0.22
Mn	0.00–0.45	0.06	0.08
Zn	0.02–1.32	0.17	0.33
Li	0.01–1.00	0.20	0.18
H	2.67–4.56	3.32	0.50
Al – ½ Li + ½ Ti	17.62–18.04	17.81	0.12
R ²⁺ + Li + Ti	3.59–4.53	4.20	0.26

* Analyses are from Holdaway et al. (1986b) and Dyar et al. (1991). Analyses with indications of high Fe³⁺ (Holdaway et al., 1986b) or >0.2 Fe³⁺ (Dyar et al., 1991) and those which did not include Li or H are excluded. For specimen 6-3, a Jan., 1991, ion probe analysis of 0.99% Li₂O was used (Richard Hervig and M. J. Holdaway, unpublished data).

** Averages were multiplied by 1.00073 to bring total charge to exactly 96.0.

† For specimens not analyzed by Mössbauer, determined by multiplying total Fe by 0.965 (see text).

‡ For specimens not analyzed by Mössbauer, determined by multiplying total Fe by 0.035 (see text).

be used to estimate the ferric content of staurolite that grew under reduced and oxidized conditions, respectively. No more precise estimate is possible at present because of the 3% error of resolved spectral doublets in the analyses.

Even though the synthetic staurolite samples all grew under conditions at least as reducing as the QFM O buffer, their average Fe³⁺ is $8 \pm 4\%$ of total Fe (Dyar et al., 1991). This apparent deviation from the composition of natural reduced staurolite may have resulted in part from the less precise nature of the data. (Small sample quantities of synthetic staurolite produced lower quality data than the natural specimens for which abundant sample was available.) Also, that doublet 6 was never resolved in synthetic staurolite meant that doublet 5 (Fe³⁺) was always resolved and therefore may have given higher averages.

SITE ASSIGNMENTS IN STAUROLITE

To arrive at the best possible site assignments, we will consider first the chemical and Mössbauer results and

then the crystal structure results, and finally determine site assignments consistent with all data.

Chemical data

Table 2 summarizes the ranges and averages of the various ions in staurolite with low Fe³⁺. Only staurolite for which H and Li have been analyzed was used in order to maximize the accuracy of the stoichiometry. The information on Fe³⁺ and the larger number of samples makes this a better data set than that given by Holdaway et al. (1986b). The ratio of the standard deviation to the average gives a good indication of the degree of variability of each ion. The information of Table 2 is useful in resolving the site assignments for staurolite and in determining chemical end-member formulas, as discussed below.

Mössbauer data

Dyar et al. (1991) have made site assignments for Fe²⁺ and Fe³⁺ in staurolite that are generally consistent with previous Mössbauer studies and structure refinements. Their Mössbauer values are averaged in Table 3, where the staurolite samples are grouped in four categories: (1) natural staurolite with 2.7–3.4 H, (2) natural staurolite with 4.0–4.6 H, (3) all natural staurolite, and (4) synthetic staurolite (unknown H). As stated above, only five of six doublets could be resolved in any given specimen. The occupancy assigned to the unresolved doublet (commonly either 5 or 6) was arbitrarily assumed to be 3%, slightly below the detection limit (Dyar et al., 1991). An alternative threshold value, 1% less than the minimum percent observed for the site or specimen, is also shown on Table 3 for the natural staurolite. The values were normalized so that Fe²⁺ occupancies sum to 100%. Some normalization procedure was necessitated by the assumption of threshold occupancies.

The four groups of staurolite samples show very similar average percent area for a given Mössbauer doublet. The exceptions occur in the synthetic staurolite, which shows higher percents of Mössbauer doublet 5 (Fe³⁺, discussed above) and doublets 1–3 and unresolved doublet 6. It is not possible to tell whether this effect is the result of lower content of ions for doublet 6 or higher content of ions for doublet 5. Because the lowest detected occupancy of doublet 6 is 7% (Dyar et al., 1991), some of the synthetic

TABLE 3. Average percents of Fe in various sites, based on total Fe²⁺ = 100%*

Doublet**	Site	2.7–3.4 H (17 spec.)	4.0–4.6 H (6 spec.)	All natural (23 spec.)	All natural† (23 spec.)	Synthetic (12 spec.)
1–3	T2	82.6 (2.6)	81.5 (2.0)	82.3 (2.4)	81.5 (1.7)	85.3 (4.1)
4	M1–M4	10.9 (1.5)	11.0 (1.1)	10.9 (1.4)	10.8 (1.3)	11.5 (4.1)
5	T2	5.5 (3.2)	3.7 (1.7)	5.1 (2.9)	4.9 (2.8)	8.2 (3.8)
6	?	6.4 (3.6)	7.6 (2.3)	6.7 (3.3)	7.7 (2.3)	3.2‡

* A threshold value of 3% was assumed for unresolved doublets before recalculation of Fe²⁺ = 100%. Numbers in parentheses are 1 σ , calculated from analyzed sample population. Data from Dyar et al. (1991).

** Designations of Dyar et al. (1991).

† For this column a threshold value 1% less than any other resolved peak for the site and the specimen was assumed for unresolved doublets.

‡ Doublet 6 was not resolved for any synthetic specimen.

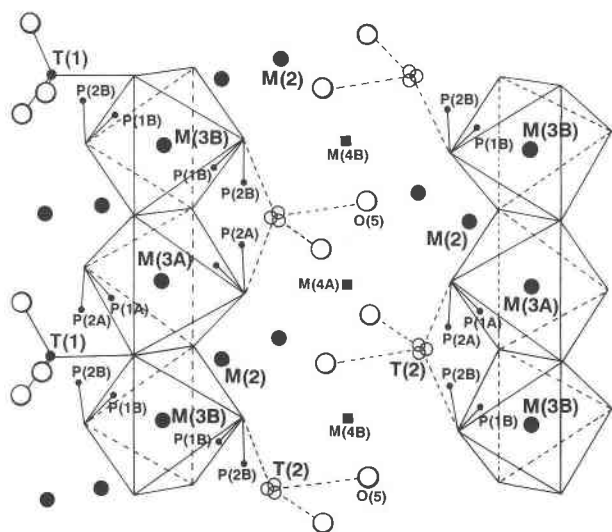


Fig. 1. Diagram of a portion of the staurolite structure showing octahedral Al sites, M2 and M3, the octahedral Fe site, M4, the tetrahedral Si site, T1, the subsites of the tetrahedral Fe site, T2, and the H sites, P1A, etc.

samples might well have greater than 3% of Fe corresponding to doublet 6 and thus a lower percent of ions for doublets 1–3.

A portion of the staurolite structure is illustrated in Figure 1. In this work, we use the redefined site nomenclature of Hawthorne et al. (manuscripts a and b, in preparation) for cation sites and the redefined site nomenclature of Dyar et al. (1991) for the proton sites. The reader is referred to the structure diagrams of Hawthorne et al. for additional structural details. Fe site assignments based on Mössbauer work are discussed below.

T2. Doublets 1–3 are interpreted as subsites of T2 (Dyar et al., 1991). About 82% of Fe^{2+} is distributed on these three subsites (Table 3). The subsites probably correspond to the T2 subsites originally identified by Smith (1968, his ^{57}Fe), and they presumably relate to H occupancy or vacancy of the adjacent proton sites (Fig. 1).

Doublet 5 is the only one discussed by Dyar et al. (1991) that is definitely Fe^{3+} . They suggest that a variable amount of Fe^{3+} replaces Al in tetrahedral sites. On the basis of the structural analyses of Hawthorne et al. (manuscript a, in preparation) discussed below, this tetrahedral Fe is probably also in the T2 rather than the T1 (Si) site.

M1–M4. Doublet 4 is that of octahedral Fe^{2+} (which may be in any or all of the octahedral sites), M1–M3 (the Al sites), or M4 (the U site) (Dyar et al., 1991). It contains an average of about 11% of Fe^{2+} (Table 3).

Charge transfer. Doublet 6 (averaging 7% in natural specimens, Table 3) is a possible charge transfer doublet (Dyar et al., 1991). Charge transfer is not possible between adjacent T2 sites because they are too far apart, and it is not likely between adjacent T2 and M4 sites because they are not simultaneously occupied (Hawthorne et al., manuscripts a and b, in preparation). It is

possible that there is charge transfer between adjacent T2 and M1–M3 sites. This is equivalent to assigning half the occupancy of doublet 6 to tetrahedral and half to octahedral sites.

Summary of Fe site data. The Mössbauer data suggest that on average about 86% of total Fe is tetrahedral and 14% is octahedral (Table 3). This figure is determined by assigning the charge transfer Fe half to T2 and half to M1–M3. Octahedral Fe is then specified as Fe in M1–M4 over total Fe (doublet 4 + half of doublet 6 over the sum of all doublets, assuming that unresolved doublets have 3% area).

Dilution in Fe sites by other ions. The possibility that all R^{2+} , Li, and Ti behave as a single group of ions (Table 2; Holdaway et al., 1986b) and that a natural staurolite sample may be produced from an Fe-end-member staurolite by equivalent dilution of Fe^{2+} by other R^{2+} , Li, and Ti in all the Fe^{2+} sites was partially tested with a York (1966) linear regression on natural staurolite samples. (For the purpose of these regressions, charge transfer Fe is considered as Fe^{2+} .) Fe^{2+} contents from Mössbauer doublets were regressed against total Fe^{2+} , each divided by total $\text{R}^{2+} + \text{Li} + \text{Ti}$, using Mössbauer data from Dyar et al. (1991). If Fe is being diluted equally in all the sites that it occupies, the slopes of the regressions should be $\text{T2} = 0.82 \pm 0.02$, $\text{M1–M4} = 0.11 \pm 0.01$, charge transfer = 0.07 ± 0.03 (Table 3). The actual slopes (Fig. 2) are $\text{T2} = 0.76 \pm 0.03$ and $\text{M1–M4} = 0.09 \pm 0.03$. There is considerable scatter in the data for M1–M4 resulting from Mössbauer error, but the trend of lower octahedral Fe with lower total Fe^{2+} is apparent and is observed for all compositional variants. The occupancies for charge transfer (doublet 6) cannot be regressed meaningfully because doublet 6 could not be resolved in ten of 23 specimens; however, five of these unresolved doublets are from samples with $\text{Fe}^{2+}/(\text{R}^{2+} + \text{Li} + \text{Ti})$ less than 0.68, and all 13 samples with resolved doublet 6 were on samples with $\text{Fe}^{2+}/(\text{R}^{2+} + \text{Li} + \text{Ti})$ greater than 0.68, suggesting that charge transfer Fe site occupancy also decreases with decreasing total Fe^{2+} . These results indicate that each Mössbauer group of Fe sites, with the possible exception of the charge transfer Fe, is being reduced in Fe content in roughly the correct ratio for equal partitioning of Fe^{2+} between the groups.

The regressions discussed above provide a necessary but not sufficient test of the hypothesis of equal dilution of Fe by other $\text{R}^{2+} + \text{Ti} + \text{Li}$ in individual sites. As discussed below, the crystal structure refinements show that partitioning of Fe^{2+} between octahedral sites is not equal.

Crystal structure data

Hawthorne et al. (manuscript a, in preparation) used 42 single crystal structure refinements of a wide variety of known staurolite compositions to determine site occupancies in terms of Si, Al, Mg, Fe^* (Fe^{2+} , Fe^{3+} , Mn, Ti, and trace transition metals), Zn, and Li. Table 4, column 2 summarizes these site occupancies for average staurolite.

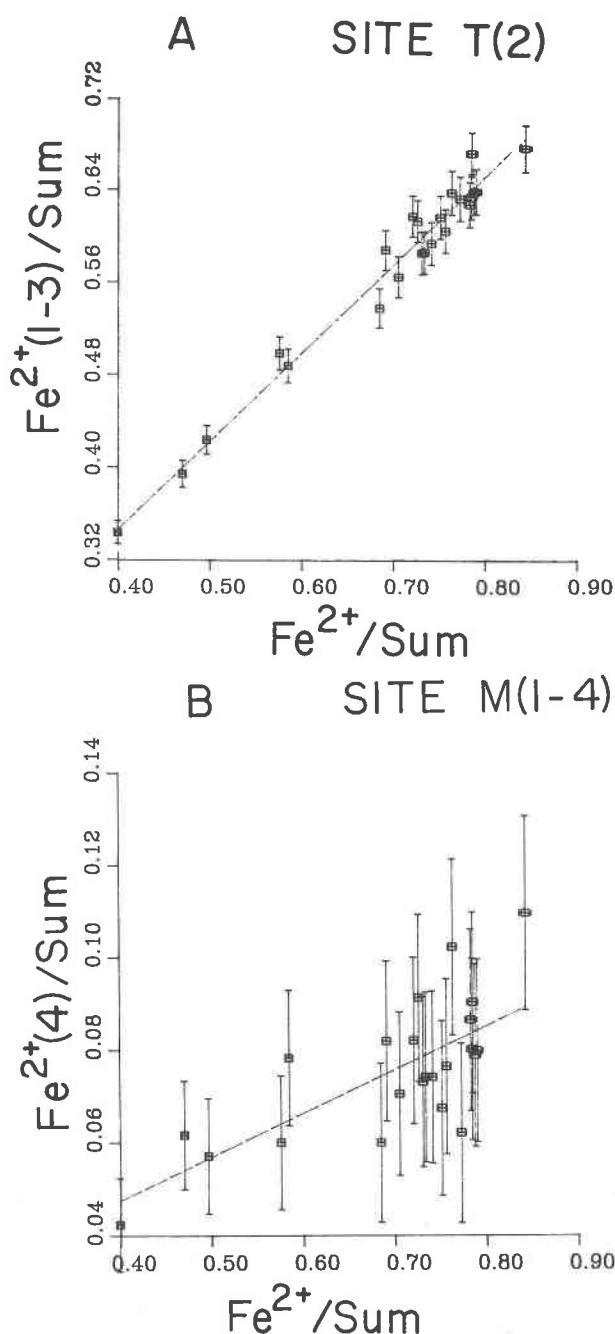


Fig. 2. York (1966) regressions of Fe^{2+} doublet content against total Fe^{2+} to suggest that Fe^{2+} decreases relative to other $\text{R}^{2+} + \text{Li} + \text{Ti}$ in each Mössbauer group of sites as total Fe^{2+} decreases. All values are normalized to $\text{R}^{2+} + \text{Li} + \text{Ti}$ (= sum). (A) Fe doublets 1-3, site T2. (B) Fe doublet 4, sites M1-M4. Fe doublet 6 (possible charge transfer) cannot be regressed because in ten of 23 specimens it was not resolved.

TABLE 4. Site occupancies based on crystal structure refinements and Mössbauer data

Site, element**	Structure average†	Modified, see text‡	Chemical average§	Si, Al, Fe^{2+} only
M1 Al	7.70(9)	7.70	7.70	7.70
Mg	0.22(9)	0.22	0.20	
Fe^* , Fe^{2+}	0.08(5)	0.08	0.10	0.30
M2 Al	7.80(7)	7.80	7.80	7.80
Mg	0.06(3)	0.06	0.05	
Fe^* , Fe^{2+}	0.14(7)	0.14	0.15	0.20
M3 Al	1.83(11)	1.83	1.81	1.81
Mg	0.10(5)	0.10	0.09	
Fe^* , Fe^{2+}	0.02(4)	0.02	0.03	0.12
□	0.05(9)	0.05	0.07	0.07
M4 Fe^* , Fe^{2+}	0.16(9)	0.14	0.16	0.18
Zn		0.01	0.01	
Li		0.01	0.01	
□	3.84(9)	3.84	3.82	3.82
T1 Si	7.60(10)	7.60	7.64	7.64
Al	0.40(10)	0.40	0.36	0.36
T2 Fe^* , Fe^{2+}	2.73(41)	2.49	2.54	3.40
Mg	0.48(21)	0.48	0.35	
Zn	0.21(37)	0.20	0.16	
Li	0.16(9)	0.15	0.19	
Ti		0.09	0.11	
Mn		0.06	0.06	
Al	0.17(15)	0.17	0.13	0.24
Fe^{3+}		0.11	0.10	
□	0.32(17)	0.32	0.36	0.36

** $\text{Fe}^* = \text{Fe}^{2+} + \text{Fe}^{3+} + \text{Ti} + \text{Mn}$, and applies only to the first column of data. A vacancy of 2 ions exists for M3, in addition to that shown here.

† Average site occupancies of Hawthorne et al. (manuscript a, in preparation); standard deviation in parentheses.

‡ Average site occupancies of Hawthorne et al. (manuscript a, in preparation) modified by interpretation of Mössbauer results (see text).

§ Average chemical data of Table 2 assigned to site occupancies based on procedure and intersite K_s values given in text.

|| Substitutions of Table 5 applied to previous column to determine chemical Si, Al, Fe^{2+} end-member.

predominantly occupied by Al but contain small amounts of Mg and Fe^* , which may be estimated by assuming that only Al, Mg, and Fe^* reside in the sites. In addition the T1 site is occupied only by Si and Al, and contains no Fe^* . Also important is the fact that all cation sites are fully occupied except M3, M4, and T2. Occupancy of M4 is coupled with half the vacancy that occurs in adjacent T2, and average vacancy in M3 above 2 is a fraction of the vacancy in T2. The combined T2-M4 and M3 vacancies are charge balanced by H in appropriate sites.

We assign Fe^{3+} to T2, since Mössbauer results (above) show it to be tetrahedral and structure determinations indicate the absence of Fe in T1. We make the simplifying assumption that staurolite is fully disordered at its T of formation. This seems reasonable when one considers that some staurolite crystals studied by Hawthorne et al. (manuscript a, in preparation) are fully disordered even at room T .

Synthesis of results

The Mössbauer results suggest some refinements to the crystal structure data. Figure 2 shows that low-Fe staurolite has reduced octahedral Fe^{2+} , even when the main diluting ion is Zn or Li. To reduce octahedral Fe in such staurolite samples, we modify the site assignments of

lite, determined by first averaging occupancies of each crystal of a sample and then averaging these averages. A high-Mg staurolite sample was excluded from the average. Their work shows clearly that the M1-M3 sites are

Hawthorne et al. (manuscript a, in preparation) to partition Fe, Zn, and Li equally between T2 and M4. For average staurolite (Table 4, columns 2 and 3) this has a trivial effect, but for Zn- and Li-rich staurolite it adequately explains Figure 2. In all staurolite samples, the effect is small enough to go undetected in crystal structure analysis. Thus, whereas total octahedral Fe is diluted about equally with tetrahedral Fe (Fig. 2), the main diluting ions appear to depend on the specific octahedral site, with Mg diluting Fe in M1–M3 and Zn and Li diluting Fe in M4.

The task remaining is to assign sites to the ions Mn and Ti, which are sufficiently abundant to warrant concern. Trace transition metals (Cr^{3+} , Co) are not considered here. In reality, each ion may be partitioned between the four octahedral and two tetrahedral sites. However, because the amounts of Ti and Mn are small, assignment of each to a single site will introduce no significant error. Reasonable possibilities are (1) assign Mn and Ti to the dominant Fe site, T2 so that Fe^* becomes Fe^{2+} in the M1–M3 sites; (2) assign Mn, the largest ion, to the largest site, M4 (see also Smith, 1968), and Ti, the smallest ion, to the smallest available site, M2; or (3) some combination of these two approaches. If Mn and Ti are assigned to the T2 site (case 1), the Hawthorne et al. (manuscript a, in preparation) crystal structure refinements (Table 4, column 2) give 13% of the Fe in octahedral sites, and the chemical analyses from Table 2 (recast in Table 4, column 3) give 15% of the Fe in octahedral sites. If the Mn and Ti are assigned to octahedral sites (case 2), the Hawthorne et al. (manuscript a, in preparation) analyses give 8% of the Fe in octahedral sites, and the analyses from Table 2 give 9% of the Fe in octahedral sites. The Mössbauer data (discussed above) indicate that about 14% of the Fe is octahedral, suggesting that case 1 is the appropriate scenario for Mn and Ti. Thus, it appears that Ti and Mn tend to concentrate where most of the Fe is, in the T2 site. An alternative assignment, which cannot be entirely ruled out, is Ti to the small M2 site and Mn to the T2 site. This would give 10% of the Fe in octahedral sites from the crystal structure data and 11% of the Fe in octahedral sites from the chemical data. To produce optimum agreement between Mössbauer and structural data, we assign Mn and Ti in Table 4 on the basis of case 1.

With the above structural assignments, it becomes possible to formulate guidelines for assigning site occupancies for a complete staurolite chemical analysis and stoichiometry on the basis of 48–O atoms. To do this, we assume Al and R^{2+} occupancies in M1–M3, partitioning of Mg and Fe^{2+} between T2 and M1–M3 sites, and partitioning of vacancies as determined by Hawthorne et al. (manuscript a, in preparation) and expressed as an average in Table 4, column 2, as modified above. Al occupancies of sites M1–M3 are very nearly constant, and whereas partitioning of Mg and Fe^{2+} and vacancies varies considerably in the refinements of Hawthorne et al. (manuscript a, in preparation), much of the variation can reasonably be ascribed to analytical error. With these assumptions, the guidelines are as follows: (1) Determine

total number of vacancies by subtracting cations from 30. This vacancy is ${}^{\text{T2}}\square + {}^{\text{M3}}\square - {}^{\text{M4}}\text{occupancy}$. Assign vacancies so that occupancy of nominally vacant M4 equals half of the vacancy of T2; vacancy in M3 (of more than two) is determined by $K_d = 3 = {}^{\text{T2}}[\square/(2 - \square)] \cdot {}^{\text{M3}}[(1 - \square)/\square]$ (based on data of Hawthorne et al., manuscript a, in preparation). (2) Assign ($\text{Fe}^{2+} + \text{Mg}$) of 0.30 to M1, 0.20 to M2, 0.12 to M3, and the remainder provisionally to T2. (3) Assign Al as 7.70 for M1, 7.80 for M2, the amount needed for M3, $8 - \text{Si}$, for T1 and the remainder for T2. (4) Assign all Zn, Li, Fe^{3+} , Ti, and Mn provisionally to T2. (5) Fill the previously determined occupancy of M4 with $\text{Fe}^{2+} + \text{Zn} + \text{Li}$ from T2 so that they partition equally between T2 and M4. (6) Partition all Mg and Fe^{2+} (excluding Fe^{2+} in M4) between T2 and M1–M3 using partition coefficients ${}^{\text{T2}}(\text{Fe}^{2+}/\text{Mg}) \cdot {}^{\text{x}}(\text{Mg}/\text{Fe}^{2+})$ of 14.5 between T2 and M1, 2.4 between T2 and M2, and 26 between T2 and M3, or using a bulk partition coefficient of 8.5 between T2 and M1–M3. It is not necessary to assign H specifically to sites because in activity models and entropy calculations H can be assumed to couple with other substitutions. This approach provides the best possible site assignments for staurolite without a crystal structure refinement. It should not be used on staurolite with $\text{Mg} > 1.6$ ions pfu because Mg behaves anomalously in such staurolite samples (Hawthorne et al., manuscript a, in preparation). The above method was used to assign sites for the average low- Fe^{3+} staurolite of Table 2, as shown in Table 4 (column 4).

The assignment of more than two vacancies in M3 requires some discussion. The estimate of a K_d of 3 between T2 and M3 vacancies (above) is an approximation based on limited data of Hawthorne et al. (manuscript a, in preparation) in which high-H staurolite has higher vacancy and lower Al occupancy of M3 than low-H staurolite, but almost all staurolite samples have some M3 vacancy content. This reduced occupancy is not reflected in reduced total Al (or Al + Si) for H-rich staurolite. The increased M3 vacancy content is required by bond valence considerations in order for H to increase above 4 (Hawthorne et al., manuscript b, in preparation). Apparently the increased M3 vacancy content is compensated by substitution of Al for R^{2+} in T2. In this way total Al + Si remains constant and increased H is chemically balanced only by decreased R^{2+} . These concepts require further study.

STAUROLITE END-MEMBER FORMULAS

Hawthorne et al. (manuscript b, in preparation) have demonstrated that the additive stoichiometric Fe^{2+} end-member formula for staurolite is hypothetical $\text{H}_2\text{Fe}_4\text{Al}_{18}\text{Si}_8\text{O}_{48}$ and that most deviations from this long-range charge-balanced formula are designed to promote short-range charge balance by increasing H. Most of the heterovalent substitutions reduce cation charge to allow for this increased H. It is now clear that this formula must be used as the thermodynamic end-member formula even though it is never approached in nature or (presumably)

in synthetic studies. Its only disorder entropy is randomness introduced by whether M3A or M3B is occupied, since M3 is statistically 50% occupied in stoichiometric staurolite (Hawthorne et al., manuscript a, in preparation). All natural and synthetic staurolite samples must be related to this end-member formula by mole fraction (activity) corrections. However, practical chemical end-member formulas for staurolite are also useful because (1) they enable us to determine the formulas of staurolite produced in experimental reaction studies of simple systems and hence to use such studies to retrieve thermodynamic data, and (2) they allow us to regress volume data on natural staurolite against chemical composition in order to determine molar volume of the chemical and stoichiometric end-members.

In this approach, we determine chemical end-member formulas that show average content of Si and Al, which are nearly constant. By accounting for the most important chemical substitutions, one can achieve electrically neutral formulas that can easily be applied to real staurolite. Table 5 gives a practical list of the various ions and their chemical substitutions. Most of the substitutions are reasonably well documented. Some of the substitutions in Table 5 are algebraic sums of substitutions given by Hawthorne et al. (manuscript b, in preparation). This is because all of the H variation in Table 5 is accomplished by substitution 5. The Ti substitution is an assumption based on analogy with the Li substitution; it is suggested that at constant H, Ti (like Li) is charge balanced by changes in Al content on T2. For both Li and Ti, this is probably an approximation. The T2 and M4 sites, which contain most of the $R^{2+} + Li + Ti$, share the characteristic of partial occupancy. The existence of these vacancies and the variable amounts of vacancies in these sites allow for substitutions 3, 4, and 5 in Table 5.

It is important to note that the proposed chemical end-members take into account only the substitutions given in Table 5. Variation in Al-Si solid solution is ignored. It can be seen (Table 2) that Al (corrected for Li and Ti substitution) and Si are nearly constant in most staurolite samples, being only slightly more variable than would be predicted by analytical error. Si standard deviation is 0.07 pfu, whereas calculated analytical error is 0.04; $Al - \frac{1}{3} Li + \frac{2}{3} Ti$ standard deviation is 0.12, whereas calculated analytical error is 0.09 (Table 2; Holdaway et al., 1986b, their Table 5). All of the analyzed staurolite samples used for Table 2 coexisted with quartz. Grew and Sandiford (1984) showed that some staurolite samples that formed in silica-undersaturated conditions contain less Si than the range given here. Thus variations in Si in staurolite that coexists with quartz are difficult to detect analytically. The formulas given below may be appropriately modified for silica-undersaturated rocks.

End-member formulas that are charge balanced and free of Fe^{3+} were derived using substitutions 1–4 (Table 5) for fixed H values (substitution 5), based on data from Table 2 (also seen in Table 4, column 4): $H_3Fe_{4.35}Al_{17.90}Si_{7.65}O_{48}$, $H_{3.5}Fe_{4.10}Al_{17.90}Si_{7.65}O_{48}$, and $H_4Fe_{3.85}Al_{17.90}Si_{7.65}O_{48}$. For

TABLE 5. Important substitutions for determining staurolite chemical end-member formulas

No.	Substitution	Sites	References*
1	$Fe^{2+} = Mg = Zn = Mn$	T2, M1–M4	1, 4, 5, 6
2	$Al = Fe^{3+}$	T2	1, 4, 5, 6
3	$Fe^{2+} + \frac{1}{3} \square = Li + \frac{1}{3} Al$	T2, M4	2, 4, 5, 6
4	$Fe^{2+} + \frac{2}{3} Al = Ti + \frac{2}{3} \square$	T2	1, 3, 5, 6
5	$Fe^{2+} + 2 \square = \square + 2 H$	T2, M4, H sites	1, 5

Note: These substitutions are arranged in such a way as to relate all H variation to substitution 5. If Al-Si solid solution were allowed to vary, it also might relate to H variation.

* 1—Holdaway et al. (1986b); 2—Dutrow et al. (1986); 3—Ward (1984); 4—Dyar et al. (1991); 5—Hawthorne et al. (manuscripts a and b, in preparation); 6—this report.

these formulas the Al value is average $Al - \frac{1}{3} Li + \frac{2}{3} Ti + Fe^{3+}$, and the Fe value is average $R^{2+} + Li + Ti$ corrected for substitution 5 (Tables 2 and 5). Additional 3 H chemical end-members that are quantitatively important include Mg, Zn, and Li staurolite, each with 4.35 Mg, Zn, or Li. At high concentrations of these ions, the stoichiometry probably changes as a result of differing degrees of replacement of Al by Mg, Zn, or Li in M1–M3 (Table 4). As a result of substitution 3 (Table 5) the Li end-member becomes $H_3Li_{4.35}Al_{19.35}Si_{7.65}O_{48}$. As Li increases, charge balance may also be accomplished by increase in Si relative to Al in T1 and some increase in Al content of M3. Whereas Mg and Zn end-members have been synthesized (Schreyer and Seifert, 1969; Griffen, 1981), this Li end-member appears to be unstable, possibly because of the high Al required (Dutrow, 1991). Ti and Mn end-members may also be written, but the extent of solid solution of these is very limited. The chemical end-members given here are similar to those given by Holdaway et al. (1986b), but they are more accurate because of the additional analyses and information on Fe^{3+} (Dyar et al., 1991).

STOICHIOMETRY FROM CHEMICAL ANALYSES

Because of the nonstoichiometric nature of both natural and synthetic staurolite and because staurolite is very rarely analyzed comprehensively (to our knowledge there are only 21 natural staurolite samples in which all cations and H have been analyzed), it is important to find ways to determine staurolite stoichiometry from analyses that typically do not include Fe^{3+} , Li, and H determinations. Holdaway et al. (1986b, p. 1155) made two suggestions: (1) For staurolite that coexists with biotite or garnet, assume average values of H and Li of 3.06 and 0.2 ions, respectively. (2) For staurolite that formed under reducing conditions, assume $Si + Al = 25.53$. These suggestions were made without benefit of Fe_2O_3 determinations.

On the basis of additional data, a relatively complicated, but more complete and more accurate, scheme for determination of staurolite stoichiometry and estimation of H content is proposed. We rely on the substitutions of Table 5 and the average data of Table 2. The sum of $Si + Al - \frac{1}{3} Li + \frac{2}{3} Ti + Fe^{3+}$ is very nearly constant in

staurolite analyzed for all cations and other staurolite whose Fe_2O_3 content can be readily estimated because it formed under reducing conditions (Table 2; Holdaway et al., 1986b, Table 5). The best estimate for this value is 25.55 ($= 7.64 + 17.81 + 0.10$, Table 2). Thus the sum of $\text{Si} + \text{Al} - \frac{1}{3}\text{Li} + \frac{2}{3}\text{Ti} + \text{Fe}^{3+}$ should be set at 25.55 ions pfu. If the analyses are of high quality, the sum of charge resulting from this choice of stoichiometry may be subtracted from 96 to yield a rough estimate for H. For example, H estimates were necessitated for two of the staurolite samples studied by Dyar et al. (1991), and the results were consistent with the H measurements made on samples from the same localities with the same mineral assemblages. For analyses in which values were normalized to standards analyzed at regular intervals, Holdaway et al. (1988) estimated 1σ error for H of 0.4 ions pfu using this method.

If Fe^{3+} is not known, it can be estimated according to the methods given in the section above on Fe^{3+} in staurolite (3.5% of Fe is Fe^{3+} in reduced staurolite, 7% of Fe is Fe^{3+} in staurolite coexisting with hematite-ilmenite solid solution $>10\%$ hematite). If Li is not known, it can be estimated at about 0.2 ions. The 27 analyses given by Holdaway et al. (1986b), which do not have recognizable high Li, average 0.16 ± 0.12 Li ions. Perhaps a better approach is to analyze representative staurolite samples from an area for Li with the ion probe—a procedure not practiced for routine petrology. Estimates for Li and, to a lesser extent, Fe^{3+} will correspondingly increase the error in the stoichiometry and H estimates.

If the above approach is used for staurolite stoichiometry, the average estimated H content of a group of related staurolite samples may be used to test the stoichiometry and the quality of the analyses by comparing the estimated H values of specimens from a known mineral assemblage with those obtained from complete analyses of staurolite (Holdaway et al., 1986a, 1986b; Holdaway and Goode, 1990; Dyar et al., 1991). Staurolite that formed with biotite or garnet (high ratio of R^{2+}/Al and therefore lower H in staurolite, Table 5, substitution 5) commonly have H ions near 3 pfu, whereas that which formed with only chloritoid (lower ratio of R^{2+}/Al) commonly have H values near 4. H content of staurolite coexisting with garnet or biotite as well as chloritoid is not yet known but may be intermediate between 3 and 4 as discussed below.

MODEL FOR THERMODYNAMIC MOLE FRACTION OF IRON STAUROLITE

Ideal mole fraction (activity) models for staurolite provide us with the ability to determine the mole fraction of a staurolite end-member in a given natural or synthetic staurolite sample and from this to relate natural staurolite compositions to end-member equilibrium curves or thermodynamic data. The best model for mole fraction is based on the stoichiometric end-member formula $\text{H}_2\text{Fe}_4\text{Al}_{18}\text{Si}_8\text{O}_{48}$ (Hawthorne et al., manuscript b, in preparation), takes into account the cation distributions given

in Table 4, and follows the rules given above for site occupancy. The substitution primarily responsible for T2 vacancies is substitution 5 (Table 5), and therefore H content and occupancy of M4 are coupled to these vacancies. Some of the H variation is also coupled to M3 substitution (Hawthorne et al., manuscripts a and b, in preparation). On this basis, a model for mole fraction of stoichiometric iron staurolite in a natural or synthetic staurolite is

$$X_{\text{Fe-St}}^{\text{staurolite}} = M^1 X_{\text{Al}}^8 \cdot M^2 X_{\text{Al}}^8 \cdot M^3 X_{\text{Al}}^2 \cdot T^1 X_{\text{Si}}^8 \cdot T^2 X_{\text{Fe}^{2+}}^4$$

Applying the data of Table 4, column 3, we have

$$\begin{aligned} X_{\text{Fe-St}}^{\text{staurolite}} &= \left(\frac{7.70}{8}\right)^8 \cdot \left(\frac{7.80}{8}\right)^8 \cdot M^3 X_{\text{Al}}^2 \cdot T^1 X_{\text{Si}}^8 \cdot T^2 X_{\text{Fe}^{2+}}^4 \\ &= 0.6015 M^3 X_{\text{Al}}^2 \cdot T^1 X_{\text{Si}}^8 \cdot T^2 X_{\text{Fe}^{2+}}^4 \end{aligned}$$

The value for $T^2 X_{\text{Fe}^{2+}}$ is the T2 Fe^{2+} site occupancy, as given in Table 4, column 3, divided by 4. If one wishes to determine the mole fraction of the chemical Fe end-member $\text{H}_3\text{Fe}_{4.35}\text{Al}_{17.90}\text{Si}_{7.65}\text{O}_{48}$, the value is 0.6015 $(1.86/2)^2 \cdot (7.65/8)^8 \cdot (3.65/4)^4$, or 0.2522 ($T^2 \square = 0.16$, $M^4 \text{occupancy} = 0.08$, $M^3 \square = 0.02$). If a natural staurolite sample is to be referred to this end-member instead of the stoichiometric end-member, one should divide the calculated activity by 0.2522.

APPLICATION—STAUROLITE-CHLORITOID ROCKS FROM TRUCHAS PEAKS, NEW MEXICO

As an example of the application of the approaches discussed above, we consider the staurolite-chloritoid-bearing rocks of Truchas Peaks discussed by Grambling (1983). Grambling shows that the bulk K_d of the staurolite-chloritoid pair passes through one at about 10% magnesium chloritoid component. Two disequilibrium assemblages and one assemblage with no indication of oxidation state were excluded from our analysis. In order to calculate stoichiometry, we made the following assumptions based on the results of this study: (1) Staurolite coexisting with ilmenite has 3.5% of its Fe as Fe^{3+} and that coexisting with hematite or ilmenite having a hematite component greater than 10% has 7% of its Fe as Fe^{3+} . (2) Chloritoid with ilmenite has 2% of its Fe as Fe^{3+} and that coexisting with hematite or ilmenite having hematite component greater than 10% has 4% of its Fe as Fe^{3+} . This approach provides very good overall stoichiometry for chloritoid. (3) Typical of average staurolite, the staurolite contains 0.18% Li_2O , corresponding to about 0.2 Li ions. There may well be some variability in Li in these staurolite samples, and this may contribute to some of the scatter in our results. Stoichiometry and site assignments were determined according to the methods given above. We emphasize that the estimated H values have a precision of about 1 ion pfu as a result of this approach.

The results are summarized in Table 6, tabulated in order of increasing chloritoid Mg number. Zn contents are given because high Li may go with high Zn (Holdaway

TABLE 6. Data on staurolite-chloritoid pairs, Truchas Range, New Mexico*

Specimen	Assemblage**	Cld Mg no.	Stau Zn	Est. H	Bulk K_d †	Activ. K_d ‡
77-54A	Ky-And-Sil-Ilm-Mag	0.001	0.03	5.3	0.03	0.09
76-391	Ky-And-Sil-Hem-Mag	0.010	0.10	5.5	0.34	1.07
77-208	Ky-Sil-Hem-Mag	0.025	0.89	4.0	0.17	0.42
77-342	Ky-Sil-Hem-Mag	0.032	0.95	4.4	0.14	0.32
77-187A	Gt-Ilm	0.036	0.04	3.6	0.82	2.02
77-163	Gt-Ilm	0.047	0.23	2.9	0.42	0.87
78-86B	Gt-Ilm-Mag	0.051	0.53	4.1	0.84	2.23
77-224A	Hem	0.053	0.00	4.6	0.98	2.42
78-22A	Bt-Gt-Ilm	0.105	0.00	3.9	1.08	2.22
77-154	Hem	0.105	1.17	4.5	1.02	3.21
77-126	Bt-Ilm-Gra	0.107	0.07	3.2	0.84	1.61
77-10A	Bt-Ilm	0.111	0.01	3.6	1.00	1.98
76-445	Bt-Gt-Gra	0.111	0.00	4.0	1.56	3.50
77-40-1	Ilm	0.117	0.08	4.3	1.34	2.95
77-53	Ky-And-Sil-Ilm	0.126	0.02	4.5	1.17	2.39

* Listed in order of increasing Cld Mg/(Mg + Fe) (Grambling, 1983).

** Each assemblage includes staurolite, chloritoid, and muscovite (no Mus in 77-40-1, Par in 77-163, Chl or Rut in some specimens). Ilm = Hem component $\leq 10\%$, Hem = Hem $> 10\%$, for calculation of Fe^{3+} in staurolite and chloritoid.

† $\text{Stau}(\text{Fe}^{2+}/\text{Mg})_{\text{Cld}}(\text{Mg}/\text{Fe}^{2+})$.

‡ $\text{Stau} \{ 1/2(\text{Fe}^{2+}/\text{Mg})_{\text{Cld}}(\text{Mg}/\text{Fe}^{2+}) \}$.

et al., 1986b), which might indicate that the assumed Li values for high-Zn staurolite were low in some cases. Recalling that all the staurolite samples coexist with chloritoid, we note that (1) with biotite or garnet, staurolite has $H < 4.1$; with no biotite or garnet, staurolite has $H > 4.0$, and (2) with Al silicate, staurolite has $H > 4.0$; with no Al silicate, staurolite has $H < 4.6$. These relationships may be explained by considering the ratio R^{2+}/Al produced by staurolite and coexisting minerals, as low R^{2+}/Al favors increased H in staurolite resulting from the $\text{R}^{2+}\text{H}_{-2}$ substitution. Variations in T , P , $X_{\text{H}_2\text{O}}$, Mg number, and SiO_2 activity may also affect H content of staurolite.

The bulk K_d values (Table 6) are essentially the same as those determined by Grambling without an Fe^{3+} correction, and they demonstrate clearly that there must be a T - X minimum for staurolite-quartz relative to chloritoid and aluminum silicate at about 0.1 $\text{Mg}/(\text{Mg} + \text{Fe}^{2+})$ (Grambling, 1983, his Fig. 13). The K_d values based on the mole fraction model must include only the Fe^{2+} and Mg content of T2 since all the other factors cancel out between $X_{\text{Fe-Si}}$ and $X_{\text{Mg-Si}}$. These K_d values must apply to equilibrium relations other than mass-action relations between Fe-Mg minerals. Table 6 shows that most of the mole fraction model K_d values are above one, and they only pass through one at very Fe-rich compositions. More important, the variable nature of K_d with composition still exists when the new mole fraction model is used. This indicates that the variable K_d relations cannot be a function of either Fe^{3+} - Fe^{2+} content or intersite partitioning in staurolite. A remaining possible explanation is nonideal mixing in the T2 sites (Holdaway et al., 1988; Mukhopadhyay et al., 1990); this will be considered in detail in a future communication.

SUMMARY

As a result of the recent chemical, Mössbauer, and X-ray crystal structure data, it is now possible to resolve a num-

ber of problems with staurolite to help make it a more useful mineral for petrogenetic studies:

1. In reduced rocks, about 3.5% of the Fe in staurolite is Fe^{3+} ; in more oxidized rocks, about 7% is Fe^{3+} .

2. Of the Fe^{2+} , 82% occurs on the T2 site, 11% on M1-M4 sites, and 7% is charge transfer, probably between T2 and M1-M3 sites. The Fe^{3+} resides on the T2 site probably replacing Al. In all, about 14% of the Fe is octahedral, 86% tetrahedral.

3. A combination of chemical, Mössbauer, and structural data allows for a model based on average site occupancies and intersite partitioning to assign all common ions from a chemical analysis to specific sites.

4. The stoichiometric formula on which mole fraction models and thermodynamic data should be based in $\text{H}_2\text{Fe}_4\text{Al}_{18}\text{Si}_8\text{O}_{48}$. However, chemical end-members such as $\text{H}_3\text{Fe}_{4.35}\text{Al}_{17.90}\text{Si}_{7.65}\text{O}_{48}$ are important for determining synthetic staurolite compositions and staurolite molar volumes.

5. The best staurolite stoichiometry can be obtained by assuming $\text{Si} + \text{Al} - 1/3 \text{Li} + 2/3 \text{Ti} + \text{Fe}^{3+} = 25.55$. H may then be estimated by subtracting total charge from 96.

6. A good mole fraction model for iron staurolite is based on the site occupancies and takes into account dilution of Al, Si, and Fe on all octahedral and tetrahedral sites except M4 which is coupled to T2. Because of coupling, H occupancies need not be considered.

7. Calculated stoichiometries for staurolite coexisting with chloritoid show reasonable H contents as a function of mineral assemblage and demonstrate that neither redox nor intersite partitioning in staurolite can explain the variable K_d between staurolite and chloritoid, leaving nonideal mixing on T2 as a possible explanation.

With these additional constraints, it is now possible to determine staurolite molar volumes and retrieve meaningful thermodynamic parameters from equilibrium determinations.

ACKNOWLEDGMENTS

This report represents a collaborative effort, primarily between Southern Methodist University and University of Oregon. We acknowledge NSF grants EAR-8904777 and EAR-9019277 to M.J.H. and EAR-8709359 and EAR-8816935 to M.D.D. We thank Richard Hervig (Arizona State University) for providing equipment and analytical expertise to analyze specimen 6-3 for Li_2O (Table 2). We thank Helen Lang (University of West Virginia) for providing specimens and for a thoughtful review of the initial version of the manuscript. We thank Jack Rice (University of Oregon) for providing synthetic specimens. The York regression program was written and provided by Patrick Shore (Washington University, St. Louis). Ed Grew (University of Maine) provided a constructive review. We are especially indebted to Frank Hawthorne (University of Manitoba) for providing early drafts of his two classic manuscripts on staurolite crystal structure and local order. This report has been greatly improved as a result.

REFERENCES CITED

- Alexander, V.D. (1989) Iron distribution in staurolite at room and low temperatures. *American Mineralogist*, 74, 610–619.
- Ballevre, M., Pinardon, J.L., Kienast, J.R., and Vuichard, J.P. (1989) Reversal of Fe-Mg partitioning between garnet and staurolite in eclogite-facies metapelites from the Champnoceaux nappe (Brittany, France). *Journal of Petrology*, 30, 1321–1349.
- Dutrow, B.L. (1991) The effects of Al and vacancies on Li substitution in iron staurolite: A synthesis approach. *American Mineralogist*, 76, 42–48.
- Dutrow, B.L., and Holdaway, M.J. (1989) Experimental determination of the upper thermal stability of Fe staurolite + quartz at medium pressure. *Journal of Petrology*, 30, 229–248.
- Dutrow, B.L., Holdaway, M.J., and Hinton, R.W. (1986) Lithium in staurolite and its petrologic significance. *Contributions to Mineralogy and Petrology*, 94, 496–506.
- Dyar, M.D. (1990) Mössbauer spectra of biotite from metapelites. *American Mineralogist*, 75, 656–666.
- Dyar, M.D., Perry, C.L., Rebbert, C.R., Dutrow, B.L., Holdaway, M.J., and Lang, H.M. (1991) Mössbauer spectroscopy of synthetic and naturally occurring staurolite. *American Mineralogist*, 76, 27–41.
- Grambling, J.A. (1983) Reversals in Fe-Mg partitioning between chloritoid and staurolite. *American Mineralogist*, 68, 373–388.
- Grew, E.S., and Sandiford, M. (1984) A staurolite-talc assemblage in tourmaline-phlogopite-chlorite schist from northern Victoria Land, Antarctica and its petrogenetic significance. *Contributions to Mineralogy and Petrology*, 87, 337–350.
- Griffen, D.T. (1981) Synthetic Fe/Zn staurolites and the ionic radius of Zn^{2+} . *American Mineralogist*, 66, 932–937.
- Guidotti, C.V., and Dyar, M.D. (1991) Ferric iron in metamorphic biotite and its petrologic and crystallochemical implications. *American Mineralogist*, 76, 161–175.
- Hawthorne, F.C., Ungaretti, L., Oberti, R., Caucia, F., Callegari, A., and Cannillo, C. (1991) Staurolite: Long-range ordering, short-range ordering and chemical formula. Geological Association of Canada Program with Abstracts, 16, A53.
- Holdaway, M.J., and Goodge, J.W. (1990) Rock pressure vs. fluid pressure as a controlling influence on mineral stability: An example from New Mexico. *American Mineralogist*, 75, 1043–1058.
- Holdaway, M.J., Dutrow, B.L., Borthwick, J., Shore, P.J., Harmon, R.S., and Hinton, R.W. (1986a) H content of staurolite as determined by H extraction line and ion microprobe. *American Mineralogist*, 71, 1135–1141.
- Holdaway, M.J., Dutrow, B.L., and Shore, P.J. (1986b) A model for the crystal chemistry of staurolite. *American Mineralogist*, 71, 1142–1159.
- Holdaway, M.J., Dutrow, B.L., and Hinton, R.W. (1988) Devonian and Carboniferous metamorphism in west-central Maine: The muscovite-almandine geobarometer and the staurolite problem revisited. *American Mineralogist*, 73, 20–47.
- Lang, H.M., and Rice, J.M. (1985) Regression modelling of metamorphic reactions in metapelites, Snow Peak, northern Idaho. *Journal of Petrology*, 26, 857–887.
- Lonker, S.W. (1983) The hydroxyl content of staurolite. *Contributions to Mineralogy and Petrology*, 84, 36–42.
- Mukhopadhyay, B., Holdaway, M.J., Gunst, R., and Dyar, M.D. (1990) Endmember thermochemical parameters and mixing properties of 3-hydrogen Fe-staurolite. Geological Society of America Abstracts with Programs, 22, 349.
- Pigge, L.C., and Greenwood, H.J. (1982) Internally consistent estimates of pressure and temperature: The staurolite problem. *American Journal of Science*, 282, 943–969.
- Schreyer, W., and Seifert, F. (1969) High-pressure phases in the system $\text{MgO-Al}_2\text{O}_3\text{-SiO}_2\text{-H}_2\text{O}$. *American Journal of Science*, 267-A, 407–443.
- Schreyer, W., Horrocks, P.C., and Abraham, K. (1984) High-magnesium staurolite in a sapphirine-garnet rock from the Limpopo belt, southern Africa. *Contributions to Mineralogy and Petrology*, 86, 200–207.
- Smith, J.V. (1968) The crystal structure of staurolite. *American Mineralogist*, 53, 1139–1155.
- Stahl, K., Kvich, Å., and Smith, J.V. (1988) A neutron diffraction study of hydrogen positions at 13K, domain model, and chemical composition of staurolite. *Journal of Solid State Chemistry*, 73, 362–380.
- Tagai, T., and Joswig, W. (1985) Untersuchungen der Kationenverteilung im Staurolith durch Neutronenbeugung bei 100 K. *Neues Jahrbuch für Mineralogie Monatshefte*, 97–107.
- Ward, C.M. (1984) Titanium and the color of staurolite. *American Mineralogist*, 69, 541–545.
- York, D. (1966) Least-squares fitting of a straight line. *Canadian Journal of Physics*, 44, 1079–1086.

MANUSCRIPT RECEIVED OCTOBER 10, 1990

MANUSCRIPT ACCEPTED JUNE 26, 1991